

## Mechanistic Changeover for the Water Substitution on *fac*-[(CO)<sub>3</sub>Re(H<sub>2</sub>O)<sub>3</sub>]<sup>+</sup> Revealed by High-Pressure NMR

Pascal V. Grundler,<sup>†</sup> Bernadette Salignac,<sup>†</sup> Sonia Cayemittes,<sup>†</sup> Roger Alberto,<sup>‡</sup> and André E. Merbach<sup>\*†</sup>

*Ecole Polytechnique Fédérale de Lausanne, Laboratoire de Chimie Inorganique et Bioinorganique, BCH, CH-1015 Lausanne, Switzerland, and Universität Zürich, Anorganisch-Chemisches Institut, Winterthurerstr. 190, 8057 Zürich, Switzerland*

Received August 15, 2003

The complex formation in water between the stable tricarbonyltriaqua *fac*-[(CO)<sub>3</sub>Re(H<sub>2</sub>O)<sub>3</sub>]<sup>+</sup> (**1**) complex and N- and S-donor ligands has been studied by high-pressure <sup>1</sup>H NMR. Rate and equilibrium constants for the formation of [(CO)<sub>3</sub>Re(Pyz)(H<sub>2</sub>O)<sub>2</sub>]<sup>+</sup>, [(CO)<sub>3</sub>(H<sub>2</sub>O)<sub>2</sub>Re( $\mu$ -Pyz)Re(H<sub>2</sub>O)<sub>2</sub>(CO)<sub>3</sub>]<sup>2+</sup>, [(CO)<sub>3</sub>Re(THT)(H<sub>2</sub>O)<sub>2</sub>]<sup>+</sup>, and [(CO)<sub>3</sub>Re(DMS)<sub>*n*</sub>(H<sub>2</sub>O)<sub>3-*n*</sub>]<sup>+</sup> (*n* = 1–3) (Pyz = pyrazine, THT = tetrahydrothiophene, DMS = dimethyl sulfide) have been determined and are in accord with previous results (Salignac, B.; Grundler, P. V.; Cayemittes, S.; Frey, U.; Scopelliti, R.; Merbach, A. E.; Hedinger, R.; Hegetschweiler, K.; Alberto, R.; Prinz, U.; Raabe, G.; Kölle, U.; Hall, S. *Inorg. Chem.* **2003**, *42*, 3516). The calculated interchange rate constant *k*<sub>i</sub><sup>‡</sup> (Eigen–Wilkins mechanism) increases from the hard O- and N-donors to the soft S-donors, as exemplified by the following series: TFA (trifluoroacetate) (*k*<sub>i</sub><sup>‡</sup> = 2.9 × 10<sup>-3</sup> s<sup>-1</sup>) < Br<sup>-</sup> < CH<sub>3</sub>CN < Pyz < THT < DMS < TU (thiourea) (*k*<sub>i</sub><sup>‡</sup> = 41.5 × 10<sup>-3</sup> s<sup>-1</sup>). On the other hand, *k*<sub>i</sub><sup>‡</sup> values remain close to that of water exchange *k*<sub>ex</sub> on **1** (*k*<sub>ex</sub> = 6.3 × 10<sup>-3</sup> s<sup>-1</sup>). Thus, an I<sub>d</sub> mechanism was assigned, suggesting however the possibility of a slight deviation toward an associatively activated mechanism with the S-donor ligands. Activation volumes determined by high-pressure NMR, for Pyz as  $\Delta V_{r,1}^{\ddagger} = +5.4 \pm 1.5$ ,  $\Delta V_{r,1}^{\ddagger} = +7.9 \pm 1.2$  cm<sup>3</sup> mol<sup>-1</sup>, for THT as  $\Delta V_{r,1}^{\ddagger} = -6.6 \pm 1$ ,  $\Delta V_{r,1}^{\ddagger} = -6.2 \pm 1$  cm<sup>3</sup> mol<sup>-1</sup>, and for DMS as  $\Delta V_{r,1}^{\ddagger} = -12 \pm 1$ ,  $\Delta V_{r,1}^{\ddagger} = -10 \pm 2$  cm<sup>3</sup> mol<sup>-1</sup> revealed the ambivalent character of **1** toward water substitution. Hence, these findings are interpreted as a gradual changeover of the reaction mechanism from a dissociatively activated one (I<sub>d</sub>), with the hard O- and N-donor ligands, to an associatively activated one (I<sub>a</sub>), with the soft S-donor ligands.

### Introduction

Tricarbonylrhenium complexes are remarkable owing to their stability and electrochemical, photochemical, and spectroscopic properties. Their various practical applications have promoted them to a class of key compounds, specifically within the photochemistry domain, where the most studied diimine complexes were highlighted as excellent emitters and photocatalysts.<sup>1</sup> In medical research, it has been thought for a long time that rhenium compounds, which contain the radioactive  $\beta^-$  emitting <sup>188</sup>Re nuclide, could stand

as promising candidates for radio immunotherapy. In this area, the research is mainly focused on development of new procedures for the labeling of proteins by a metal, particularly the technetium extensively used in diagnostic medicine.<sup>2</sup> However, it is the report of a few years ago of the stable tricarbonyltriaqua *fac*-[(CO)<sub>3</sub>Re(H<sub>2</sub>O)<sub>3</sub>]<sup>+</sup> (**1**) complex which significantly broadened the field of investigations with rhenium in these areas.<sup>3</sup> Also part of the emergent aqua-organometallic chemistry domain, **1** has to be related to its structural analogues [(C<sub>6</sub>H<sub>6</sub>)M(H<sub>2</sub>O)<sub>3</sub>]<sup>2+</sup> (M = Ru, Os) and [Cp<sup>\*</sup>M'(H<sub>2</sub>O)<sub>3</sub>]<sup>2+</sup> (M' = Rh<sup>III</sup>, Ir<sup>III</sup>). The exhaustive studies conducted on these half-sandwich complexes revealed two main features: the strong labilizing effect of the organic

\* To whom correspondence should be addressed. E-mail: Andre.Merbach@epfl.ch (A.E.M.).

<sup>†</sup> Ecole Polytechnique Fédérale de Lausanne.

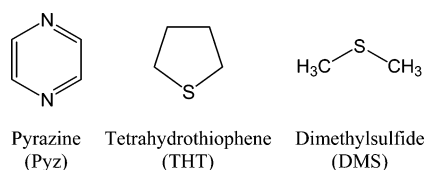
<sup>‡</sup> Universität Zürich.

(1) (a) Vogler, A.; Kunkely, H. *Coord. Chem. Rev.* **2000**, *200–202*, 991. (b) Koike, K.; Okoshi, N.; Hori, H.; Takeuchi, K.; Ishitani, O.; Tsubaki, H.; Clark, I. P.; George, M. W.; Johnson, F. P. A.; Turner, J. J. *J. Am. Chem. Soc.* **2002**, *124*, 11448–11455. (c) Sun, S.-S.; Lees, A. J. *Coord. Chem. Rev.* **2002**, *230*, 171–192.

(2) (a) Alberto, R.; Schibli, R.; Waibel, R.; Abram, U.; Schubiger, A. P. *Coord. Chem. Rev.* **1999**, *190–192*, 901. (b) Jurisson, S. S.; Lydon, J. D. *Chem. Rev.* **1999**, *99*, 2205–2218.

(3) Alberto, R.; Egli, A.; Abram, U.; Hegetschweiler, K.; Gramlich, V.; Schubiger, P. A. *J. Chem. Soc., Dalton Trans.* **1994**, 2815.

Scheme 1



ligand on the *trans* water molecules, compared to the corresponding hexaaquaions, and the  $I_d$  water exchange mechanism.<sup>4,5</sup> Nevertheless, the kinetic data available for the only other carbonylaqua complexes  $[(CO)_nRu(H_2O)_{6-n}]^{2+}$  ( $1 \leq n \leq 3$ ) are at variance with this trend since, for example, the water exchange rate on  $[(CO)_3Ru(H_2O)_3]^{2+}$  was estimated between 1 and 2 orders of magnitude lower than on  $[Ru(H_2O)_6]^{2+}$ .<sup>6</sup>

Recently, we reported the kinetic study of the water exchange on **1**, which was found to proceed with a relatively low rate constant  $k_{ex}$  as  $6.3 \times 10^{-3} s^{-1}$ .<sup>7</sup> In this study, the complex formation of **1** was performed with various ligands to estimate the response to the nucleophilicity of the entering group, a common criterion for mechanism assignment. For each ligand, the calculated interchange rate constant  $k'_i$  ( $2.9 \times 10^{-3}$  (TFA)  $< k'_i < 41.5 \times 10^{-3}$  (TU)  $s^{-1}$ ) was found close to that of water  $k_{ex}$ , the S-donor ligands being slightly more reactive. The small increase in  $k$ , from the hard trifluoroacetate anion (TFA) to the soft thiourea (TU), is in sharp contrast to the wide variation typical for associative reactions.<sup>8</sup> The rather small value of the discrimination factor  $S$  (0.3) well exemplifies this slight discrimination among nucleophiles. For the water exchange on **1**, a positive activation entropy  $\Delta S^\ddagger_{ex}$  was obtained ( $+14 \pm 10 J K^{-1} mol^{-1}$ ). These results were interpreted as indicative of a dissociative activation. However it is known that large experimental errors are inherent in the long extrapolation needed to estimate  $\Delta S^\ddagger$  values from intercepts whereas it is more obvious whether the rate constant increases or decreases as the pressure is increased, i.e., whether  $\Delta V^\ddagger$  is positive or negative. Hence, in order to unambiguously determine the complex formation mechanism of **1**, variable pressure kinetic studies have been performed and are reported here with hard N-donor and soft S-donor ligands (Pyz, THT and DMS) (Scheme 1).

## Experimental Section

**Materials.** Deuterated solvents were purchased from Aldrich and CIL. Solutions of commercially purchased  $NaCF_3SO_3$  (Aldrich) were found to be basic, due to alkaline traces. Therefore, the  $NaCF_3SO_3$  salt was neutralized by addition of  $CF_3SO_3H$ .  $HBF_4$  was freshly

prepared from  $H_2SO_4$  and  $Ba(BF_4)_2$ , which was itself prepared from  $Ba(OH)_2 \cdot 8H_2O$  and commercial aqueous  $HBF_4$ .  $Ba(BF_4)_2$  was purified according to literature methods.<sup>9</sup> All other chemicals, commercially available products of highest possible quality (Fluka, Merck, Riedel de Haën, Acros), were used without further purification.

**$[(CO)_3Re(H_2O)_3]^+$  (**1**).** The reported synthesis of **1**, in aqueous medium, is quite straightforward using the  $(NEt_4)_2[(CO)_3ReBr_3]$  compound as precursor.<sup>3</sup> The addition of 3 equiv of  $AgX$  ( $X = CF_3SO_3^-; BF_4^-$ ) to a 0.1 M HX acid solution of  $(NEt_4)_2[(CO)_3ReBr_3]$  provides solutions of **1**, after  $AgBr$  removal by filtration.

**NMR Measurements.**  $^1H$  NMR spectra were measured on Bruker ARX-400 and DPX-400 spectrometers with resonance frequencies at 400.13 MHz.  $^1H$  chemical shifts are referenced to TMS and measured with respect to the methyl group of  $NEt_4^+$  ( $\delta_{1H} = 1.25$  ppm, methyl group) or to the sodium 3-trimethylsilylpropane sulfonate internal reference. All aqueous solutions contained 10%  $D_2O$  as an internal lock substance. The temperature was controlled by a Bruker B-VT 3000 unit and measured before and after accumulations by substituting the sample with a Pt-100 resistance (accuracy:  $\pm 0.5$  K). High-pressure high-resolution NMR spectra were recorded with a home-built narrow bore probe.<sup>10</sup> Fluorobrene or tetrachloroethylene were used as pressurization liquids. The temperature was stabilized to  $\pm 0.2$  K by pumping thermostated ethanol around the high-pressure vessel.

**Kinetic Data Treatment.** Kinetic experiments were conducted by monitoring the evolution of NMR signals with time. The NMR integrals were obtained by fitting the signals to a Lorentzian function with the program NMRICMA 2.8 for MATLAB.<sup>11</sup> The time dependent concentrations were extracted from the integrals and the parameters of the appropriate equations were least-squares fitted to the experimental data using the programs VISUALISEUR 2.3.0 and OPTIMISEUR 2.3.0 for MATLAB<sup>12</sup> as well as the SCIEN-TIST<sup>13</sup> program.

**UV Measurements.** The spectrophotometric data were measured on a Perkin-Elmer Lambda 19 double beam spectrometer using the PECSS 4.01 software on a connected PC. 10 mm cells are used for the ambient pressure measurements. The high-pressure study was performed in 20 mm Le Noble cells with a home-built high-pressure vessel. The temperature was stabilized using a water flux produced by a Huber Ministat and controlled between the reference and the sample cell by a 100  $\Omega$  Pt resistance connected to a digital Technoterm 7600 thermometer.

**UV Data Treatment.** For the variable acidity measurements, the limiting spectra and the acidity constant  $K_a$  were obtained using the global analysis software Specfit.<sup>14</sup>

## Results

**Thermodynamics of Protonation on Pyrazine.** As we previously reported, the water exchange rate on  $[(CO)_3Re(H_2O)_3]^+$  (**1**) is not affected by the kinetic contribution of the much more reactive monohydroxo species  $[(CO)_3Re-$

(4) Stebler-Röthlisberger, M.; Hummel, W.; Pittet, P.-A.; Bürgi, H.-B.; Ludi, A.; Merbach, A. E. *Inorg. Chem.* **1988**, *27*, 1358.

(5) (a) Dadci, L.; Elias, H.; Frey, U.; Höring, A.; Koelle, U.; Merbach, A. E.; Paulus, H.; Schneider, J. S. *Inorg. Chem.* **1995**, *34*, 306. (b) Cayemittes, S.; Poth, T.; Fernandez, M. J.; Lye, P. G.; Becker, M.; Elias, H.; Merbach, A. E. *Inorg. Chem.* **1999**, *38*, 4309.

(6) Meier, U. C.; Scopelliti, R.; Solari, E.; Merbach, A. E. *Inorg. Chem.* **2000**, *39*, 3816.

(7) Salignac, B.; Grundler, P. V.; Cayemittes, S.; Frey, U.; Scopelliti, R.; Merbach, A. E.; Hedinger, R.; Hegetschweiler, K.; Alberto, R.; Prinz, U.; Raabe, G.; Kölle, U.; Hall, S. *Inorg. Chem.* **2003**, *42*, 3516.

(8) Tobe, M. L.; Burgess, J. *Inorganic Reaction Mechanisms*; Addison-Wesley Longman Ltd.: Reading, MA, 1999.

(9) Pawlenko, S. Z. *Anorg. Allg. Chem.* **1959**, *301*, 336.

(10) (a) Cusanelli, A.; Nicula-Dadci, L.; Frey, U.; Merbach, A. E. *Inorg. Chem.* **1997**, *36*, 2211. (b) Frey, U.; Helm, L.; Merbach, A. E.; Roulet, R. *Advanced Applications of NMR to Organometallic Chemistry*; Wiley & Sons: New York, 1996. (c) Frey, U.; Helm, L.; Merbach, A. E. *High Pressure Research*; Gordon and Breach: Langhorne, PA, 1990; Vol. 2, p 237.

(11) Helm, L.; Borel, A. Institut de Chimie Moléculaire et Biologique, Ecole Polytechnique Fédérale de Lausanne, Switzerland.

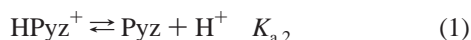
(12) Yerly, F. Institut de Chimie Moléculaire et Biologique, Ecole Polytechnique Fédérale de Lausanne, Switzerland, 1999–2001.

(13) Scientist, version 2.0; Micromath, Inc.: Salt Lake City, UT, 1995.

(14) SPECFIT; Spectrum Software Associates: Chapel Hill, NC.

(OH)(H<sub>2</sub>O)<sub>2</sub>] at  $[\text{H}^+] > 3 \times 10^{-3}$  M concentrations.<sup>7</sup> Therefore, to perform water substitution on **1**, i.e., in such acidic conditions, the N-donor pyrazine ligand (Scheme 1) is very convenient due to its acido-basic properties ( $\text{p}K_{\text{a},1} = -5.8$ ;  $\text{p}K_{\text{a},2} = 0.6$ ; 303 K;  $I = 0.1$  M)<sup>15</sup> which ensure one N site to be nonprotonated in aqueous medium and reactive for coordination. On the other hand, one should be attentive to the linker properties of pyrazine, and its derivatives, frequently used for this purpose in synthesis and often encountered as bridging ligand in rhenium–carbonyl macromolecular systems.<sup>1c,16</sup>

In view of the acido-basic nature of pyrazine in water, experiments have been conducted to determine the acid dissociation constant  $K_{\text{a},2}$  at  $I = 1$  M and 298 K (eq 1).



Spectrophotometric measurements ( $200 < \lambda < 500$  nm) were performed with solutions of pyrazine ( $2 \times 10^{-4}$  M) at variable acidity ( $10^{-7} < [\text{H}^+] < 1$  M; concentrations and not activities are used throughout the text<sup>7</sup>) in  $\text{CF}_3\text{SO}_3\text{H}$  at 298 K ( $I = 1$  M adjusted with  $\text{NaCF}_3\text{SO}_3$ ) (Figure S1). A global analysis of these data provides the limiting spectra and the acidity constant  $K_{\text{a},2}$  as  $0.15 \pm 0.03$  M (Table S1). To confirm this result, a <sup>1</sup>H NMR study was carried out with solutions of pyrazine (0.01 M) at variable acidity ( $0.01 < [\text{H}^+] < 0.59$  M) in  $\text{CF}_3\text{SO}_3\text{H}$  at 298 K ( $I = 1$  M adjusted with  $\text{NaCF}_3\text{SO}_3$ ) (Table S2). The dependence on the  $[\text{H}^+]$  concentration of the pyrazine chemical shift  $\delta$  is shown in Figure 1a.

$$\delta = \frac{\delta_{\text{Pyz}} \times K_{\text{a},2} + \delta_{\text{HPyz}} \times [\text{H}^+]}{[\text{H}^+] + K_{\text{a},2}} \quad (2)$$

Equation 2 was fitted to the experimental data leading to  $\delta_{\text{Pyz}}$  and  $\delta_{\text{HPyz}}$ , as  $8.63 \pm 0.01$  and  $9.18 \pm 0.01$  ppm, respectively, and  $K_{\text{a},2}$  as  $0.14 \pm 0.02$  M, which is in good agreement with the spectrophotometric value.

The pressure dependence ( $10 < P < 200$  MPa) of the pyrazine acidity constant  $K_{\text{a},2}$  (eq 1) has been studied at 298 K with solutions of pyrazine in  $\text{CF}_3\text{SO}_3\text{H}$  ( $I = 1$  M adjusted with  $\text{NaCF}_3\text{SO}_3$ ), by spectrophotometry ( $[\text{Pyz}] = 3 \times 10^{-4}$  M,  $[\text{H}^+] = 0.1$  M), and by <sup>1</sup>H NMR ( $[\text{Pyz}] = 0.01$  M,  $[\text{H}^+] = 0.05$  M). Increasing the pressure leads to a slight absorbance increase (Figure S2). Equation 3a,b, where  $\epsilon'$  values ( $\epsilon \times l$ , with  $\epsilon =$  molar absorptivity and  $l =$  path length) for the monoprotonated ( $\epsilon'_{\text{HPyz}}$ ) and the nonprotonated ( $\epsilon'_{\text{Pyz}}$ ) pyrazine, were fitted simultaneously for three different wavelengths (270, 275, and 280 nm) leading to the acidity constant  $K_{\text{a},2}^{298,0}$  as  $0.145 \pm 0.01$  M, the reaction

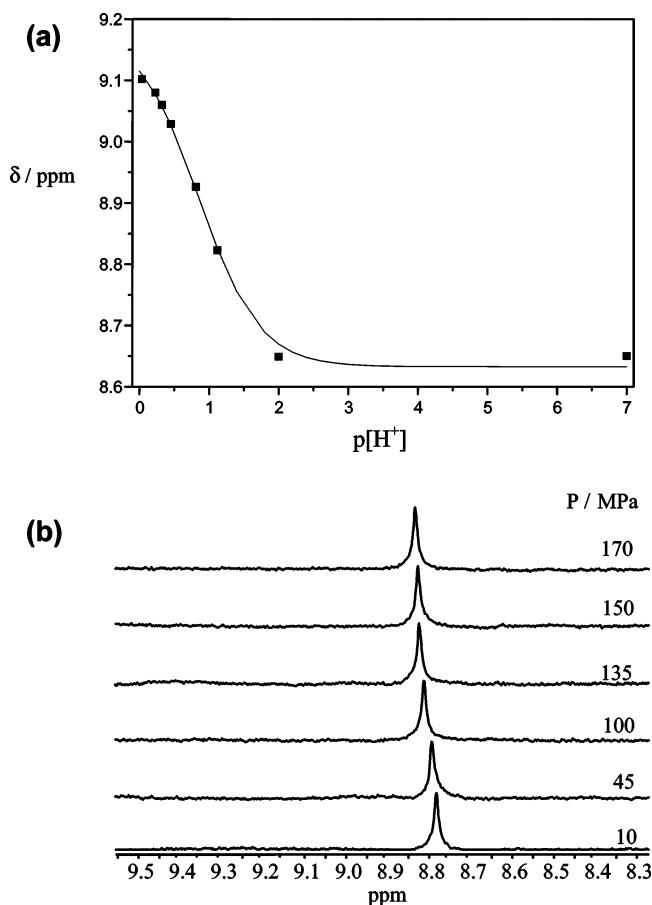


**Figure 1.** (a) <sup>1</sup>H NMR chemical shift  $\delta$  of pyrazine (0.1 M) vs  $\text{p}[\text{H}^+]$  in  $\text{CF}_3\text{SO}_3\text{H}$  ( $I = 1$  M;  $\text{NaCF}_3\text{SO}_3$ ) at 298 K. (b) Variable pressure <sup>1</sup>H NMR spectra of a solution of pyrazine 0.01 M in 0.05 M  $\text{CF}_3\text{SO}_3\text{H}$  ( $I = 1$  M;  $\text{NaCF}_3\text{SO}_3$ ) at 298 K.

volume  $\Delta V_{\text{a},2}^\circ$  as  $7.9 \pm 0.7$  cm<sup>3</sup> mol<sup>-1</sup>, as well as  $\epsilon'_{\text{HPyz}}$  and  $\epsilon'_{\text{Pyz}}$  (Table S1).

$$K_{\text{a},2}^{298,P} = K_{\text{a},2}^{298,0} \exp\left(\frac{-\Delta V_{\text{a},2}^\circ \times P}{R \times T}\right) \quad (3a)$$

$$K_{\text{a},2}^{298,P} = [\text{H}^+] \times \frac{\epsilon'_{\text{HPyz}} \times C_{\text{Pyz}} - A(P)}{A(P) - \epsilon'_{\text{Pyz}} \times C_{\text{Pyz}}} \quad (3b)$$

$$K_{\text{a},2}^{298,P} = [\text{H}^+] \times \frac{\delta_{\text{HPyz}} - \delta(P)}{\delta(P) - \delta_{\text{Pyz}}} \quad (3c)$$

Using <sup>1</sup>H NMR, a pressure increase alters slightly the chemical shift  $\delta$  of pyrazine (Figure 1b), which goes from 8.782 ppm at 10 MPa to 8.835 ppm at 170 MPa (Table S3). Equation 3a,c were fitted to the pressure dependence of  $\delta$  to give  $K_{\text{a},2}^{298,0}$  as  $0.134 \pm 0.01$  M and  $\Delta V_{\text{a},2}^\circ$  as  $6.7 \pm 0.2$  cm<sup>3</sup> mol<sup>-1</sup>.

These two  $\Delta V_{\text{a},2}^\circ$  values, which are in good agreement and close to the value reported in the literature ( $6.3$  cm<sup>3</sup> mol<sup>-1</sup>),<sup>17</sup> indicate that the protonation of the pyrazine is the favored process as the pressure increases so the molar ratio of  $\text{HPyz}^+$  in 0.01 M  $\text{CF}_3\text{SO}_3\text{H}$  rises from 7% at 0.1 MPa to 11% at 200 MPa (298 K,  $I = 1$  M).

(15) Schmidt, J. G.; Trimble, R. F. *J. Phys. Chem.* **1962**, *66*, 1063.

(16) (a) Sole, R. V.; Hupp, J. T.; Stern, C. L.; Albrecht-Schmitt, T. E. *Inorg. Chem.* **1996**, *35*, 4096–4097. (b) Rajendran, T.; Manimaran, B.; Lee, F.-Y.; Lee, G.-H.; Peng, S.-M.; Wang, C. M.; Lu, K.-L. *Inorg. Chem.* **2000**, *39*, 2016–2017. (c) Chen, X.; Femia, F. J.; Babich, J. W.; Zubieta, J. *Inorg. Chim. Acta* **2001**, *315*, 66–72. (d) Rajendran, T.; Manimaran, B.; Lee, F.-Y.; Chen, P.-C.; Lee, G.-H.; Peng, S.-M.; Chen, Y.-J.; Lu, K.-L. *J. Chem. Soc., Dalton Trans.* **2001**, 3346–3351.

(17) Conway, B. E.; Ayranci, E. *J. Chem. Thermodyn.* **1988**, *20*, 9–27.

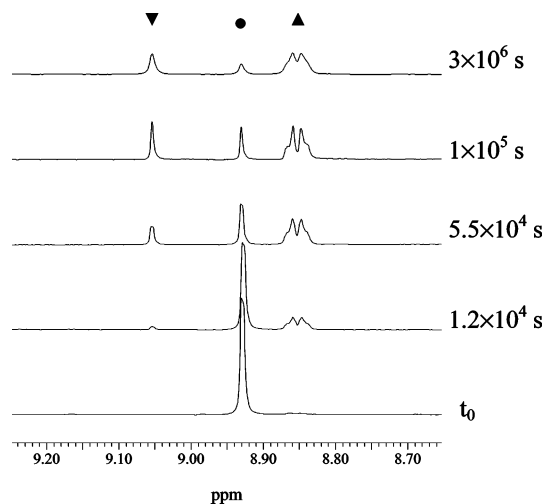


**Figure 2.**  $^1\text{H}$  NMR spectra of a solution containing initially  $[(\text{CO})_3\text{Re}(\text{H}_2\text{O})_3]^+$  (**1**) 0.05 M, pyrazine 0.01 M in  $\text{CF}_3\text{SO}_3\text{H}$  0.15 M ( $I = 1$  M;  $\text{NaCF}_3\text{SO}_3$ ) at 298 K: free pyrazine (●),  $[\text{Re}(\text{Pyz})]^+$  (▲),  $[\text{Re}(\mu\text{-Pyz})\text{Re}]^{2+}$  (▼).

**Complex Formation of  $[(\text{CO})_3\text{Re}(\text{H}_2\text{O})_3]^+$  (**1**) with the N-Donor Pyrazine Ligand.** The complex formation of  $[(\text{CO})_3\text{Re}(\text{H}_2\text{O})_3]^+$  (**1**) with pyrazine has been studied with a deficiency or an excess of ligand, compared to the 1/1 stoichiometry, by  $^1\text{H}$  NMR at 298 K and fixed ionic strength ( $I = 1$  M adjusted with  $\text{NaCF}_3\text{SO}_3$ ). The spectra (Figure 2) recorded with a solution of **1** (0.05 M) deficient in ligand (0.01 M), in 0.15 M  $\text{CF}_3\text{SO}_3\text{H}$ , exhibit the singlet of the free ligand (8.92 ppm) and, after some time, two multiplets attributed to the two types of nonequivalent protons of the pyrazine in the monocomplex  $[(\text{CO})_3\text{Re}(\text{H}_2\text{O})_2(\text{Pyz})]^+$  (8.85, 8.87 ppm) and a sharp singlet (9.06 ppm), assigned to the  $D_{2h}$  symmetric pyrazine within the dinuclear complex  $[(\text{CO})_3\text{-}(\text{H}_2\text{O})_2\text{Re}(\mu\text{-Pyz})\text{Re}(\text{H}_2\text{O})_2(\text{CO})_3]^{2+}$ . On the other hand, the spectra recorded with a solution of **1** (0.05 M) in excess of pyrazine (0.1 M), in 0.1 M  $\text{CF}_3\text{SO}_3\text{H}$ , show, as well, the signals of the mono-complex and the dinuclear species, the latter of very weak intensity, but also two additional peaks (8.65, 8.80 ppm) attributed to the bis-complex  $[(\text{CO})_3\text{Re}(\text{H}_2\text{O})(\text{Pyz})_2]^+$  (Figure S3).

**Kinetics and Thermodynamics of Water Substitution on  $[(\text{CO})_3\text{Re}(\text{H}_2\text{O})_3]^+$  (**1**) by Pyrazine at Variable Acidity.** To perform the kinetic study of the water substitution on **1** by pyrazine, experimental conditions with a deficiency of ligand have been chosen. The reaction of **1** (0.05 M) and pyrazine (0.01 M) has been followed by  $^1\text{H}$  NMR at variable  $[\text{H}^+]$  concentration ( $0.01 < [\text{H}^+] < 0.59$  M) in  $\text{CF}_3\text{SO}_3\text{H}$  at 298 K ( $I = 1$  M adjusted with  $\text{NaCF}_3\text{SO}_3$ ) (Figure 3). The spectra were recorded taking into account the relaxation delays  $T_1$  of the free and bound pyrazine, determined as 6 s and 2 s, respectively. For simplification, **1** and its mono- and dinuclear complexes with pyrazine are noted in this section as  $[\text{Re}(\text{H}_2\text{O})]^+$ ,  $[\text{Re}(\text{Pyz})]^+$ , and  $[\text{Re}(\mu\text{-Pyz})\text{Re}]^{2+}$ , respectively. The two signals of the mono-complex, at 8.85 and 8.87 ppm, appeared insensitive to varying acidity indicating that bound pyrazine is nonprotonated. The dinuclear species is observed at 9.06 ppm. The signal of the free pyrazine, of decreasing intensity, and those of bound

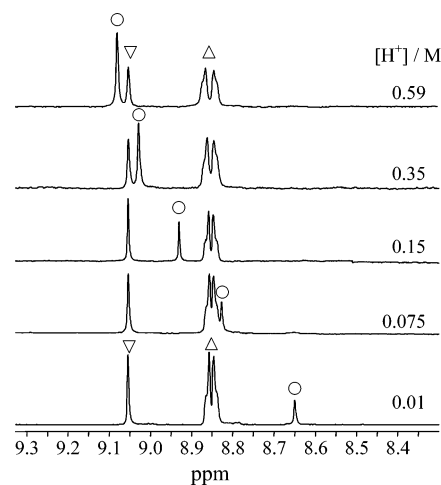


**Figure 3.** Variable acidity  $^1\text{H}$  NMR spectra of solutions containing initially  $[(\text{CO})_3\text{Re}(\text{H}_2\text{O})_3]^+$  (**1**) 0.05 M and pyrazine 0.01 M in  $\text{CF}_3\text{SO}_3\text{H}$  ( $I = 1$  M;  $\text{NaCF}_3\text{SO}_3$ ) at 298 K: pyrazine (○),  $[\text{Re}(\text{Pyz})]^+$  (△),  $[\text{Re}(\mu\text{-Pyz})\text{Re}]^{2+}$  (▽).

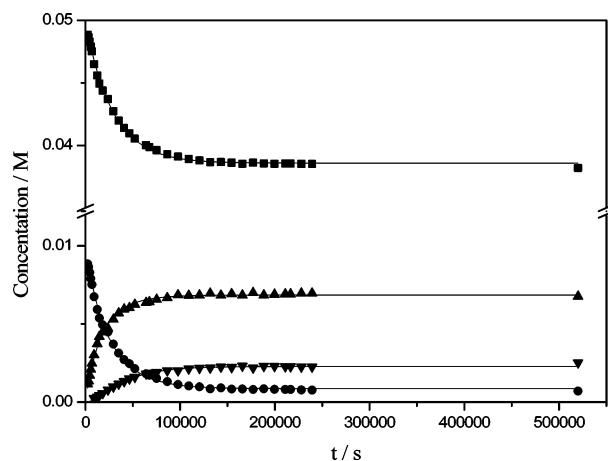
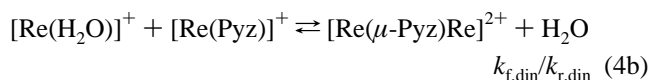


**Figure 4.** Plot, as a function of time, of the concentrations of  $[(\text{CO})_3\text{Re}(\text{H}_2\text{O})_3]^+$  (**1**) (■), free pyrazine (●),  $[\text{Re}(\text{Pyz})]^+$  (▲),  $[\text{Re}(\mu\text{-Pyz})\text{Re}]^{2+}$  (▼). Initial composition  $[(\text{CO})_3\text{Re}(\text{H}_2\text{O})_3]^+$  (**1**) 0.05 M and pyrazine 0.01 M in  $\text{CF}_3\text{SO}_3\text{H}$  0.01 M ( $I = 1$  M;  $\text{NaCF}_3\text{SO}_3$ ) at 298 K.

pyrazine, of increasing intensities, were least-squares fitted as Lorentzians, and the time dependent concentrations of the four species  $\text{HPyz}^+$ ,  $\text{Pyz}$ ,  $[\text{Re}(\text{Pyz})]^+$ , and  $[\text{Re}(\mu\text{-Pyz})\text{Re}]^{2+}$  were calculated from the obtained intensities, using  $K_{a,2}$  for pyrazine speciation, whereas that of **1** was deduced by difference (Figure 4). Assuming  $\text{Pyz}$  is the only reactive species for water substitution on **1**, second-order kinetics were applied to the experimental data of each experiment, i.e., for each  $[\text{H}^+]$  concentration (eq 4a,b).



The determined  $k_{f,\text{obs}}$ ,  $k_{r,\text{obs}}$  values were found to be  $[\text{H}^+]$  dependent whereas, as expected,  $k_{f,\text{din}}$ ,  $k_{r,\text{din}}$  were not (Table S4). Therefore, considering two kinetic pathways for  $[\text{Re}(\text{Pyz})]^+$  formation, involving either  $\text{HPyz}^+$  or  $\text{Pyz}$  (eq 5,b), linear regressions of  $k_{f,\text{obs}}$  and  $k_{r,\text{obs}}$  versus  $[\text{H}^+]$  (Figure 5), according to eq 5c, lead to the respective equilibrium and rate constants (Table 1).

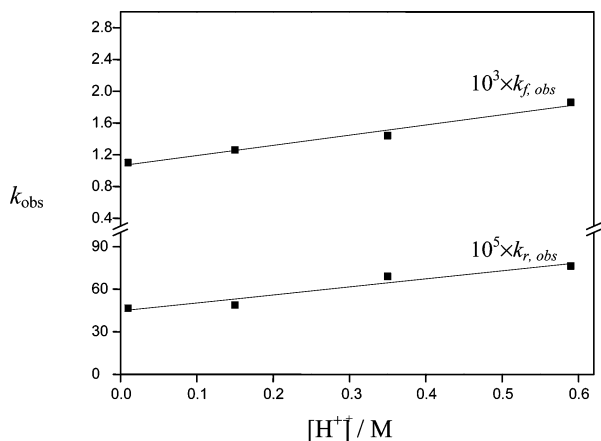
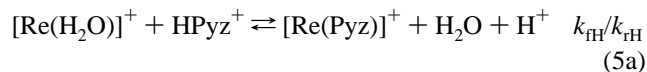


**Figure 5.** Plot as a function of  $[\text{H}^+]$  of the observed forward and reverse rate constants for the formation of  $[\text{Re}(\text{Pyz})]^+$  at 298 K ( $\text{CF}_3\text{SO}_3\text{H}$ ;  $I = 1$  M;  $\text{NaCF}_3\text{SO}_3$ ).

**Table 1.** Rate and Equilibrium Constants for the Formation of  $[(\text{CO})_3\text{Re}(\text{Pyz})(\text{H}_2\text{O})_2]^+$  and  $[(\text{CO})_3(\text{H}_2\text{O})_2\text{Re}-\text{Pyz}-\text{Re}(\text{H}_2\text{O})_2(\text{CO})_3]^{2+}$  at 298 K ( $I = 1$  M;  $\text{NaCF}_3\text{SO}_3$ )

	$\mathbf{1} + \text{Pyz} \rightleftharpoons [\text{Re}(\text{Pyz})]^+$	$\mathbf{1} + \text{HPyz}^+ \rightleftharpoons [\text{Re}(\text{Pyz})]^+ + \text{H}^+$	$\mathbf{1} + [\text{Re}(\text{Pyz})]^+ \rightleftharpoons [\text{Re}(\mu\text{-Pyz})\text{Re}]^{2+}$
$10^3 k_f^{298}/\text{M}^{-1}\text{s}^{-1}$	$1.06 \pm 0.05$	$0.187 \pm 0.020$	$0.213 \pm 0.008$
$10^5 k_r^{298}/\text{s}^{-1}$	$0.45 \pm 0.04$	$0.57 \pm 0.1^b$	$2.59 \pm 0.13$
$10^3 k_f'/\text{s}^{-1}^a$	17.7	0.68	0.77
$K^{298}/\text{M}^{-1}$	$237 \pm 15$	$33 \pm 5$	$8.2 \pm 0.2$

<sup>a</sup>  $k_f' = (k_{f,1f})/(K_{os}n_c)$  with  $1/f =$  probability factor =  $1/12$ ,  $n_c =$  coordination number = 3,  $K_{OS} = 1.1 \text{ M}^{-1}$  for charged ligands, and  $K_{OS} = 0.24 \text{ M}^{-1}$  for neutral ligands. <sup>b</sup>  $\text{M}^{-1} \text{ s}^{-1}$ .



$$k_{\text{f,obs}} = k_{\text{f},1} + k_{\text{fH}} \times ([\text{H}^+]/K_{a,2}) \quad k_{\text{r,obs}} = k_{\text{r},1} + k_{\text{rH}} \times [\text{H}^+] \quad (5c)$$

**Kinetics and Thermodynamics of Water Substitution on  $[(\text{CO})_3\text{Re}(\text{H}_2\text{O})_3]^+$  (**1**) by Pyrazine at Variable Pressure.** In order to determine the activation mode of the water substitution on **1** by pyrazine, variable pressure kinetic experiments have been performed by  $^1\text{H}$  NMR at 298 K at variable pressure ( $40 < P < 200$  MPa), using a home-built high-pressure probe.<sup>10</sup> These experiments were performed with solutions of **1** (0.05 M) with a deficiency of ligand ( $[\text{Pyz}] = 0.01$  M) in 0.01 M  $\text{CF}_3\text{SO}_3\text{H}$  ( $I = 1$  M adjusted with  $\text{NaCF}_3\text{SO}_3$ ) to avoid substitution of more than one water molecule. For each pressure studied, the time dependent concentrations of the three pyrazine-containing species (free pyrazine and mono- and dinuclear complex) were calculated from the fitted NMR intensities. For each spectrum, concentrations of  $\text{HPyz}^+$  and  $\text{Pyz}$  were calculated according to  $K_{a,2}^{298,P}$  values. However, for the analysis, the kinetic contribution of  $\text{HPyz}^+$ , which represent 11% maximum of the total pyrazine (200 MPa, 0.01 M  $\text{CF}_3\text{SO}_3\text{H}$ ), was neglected since  $\text{HPyz}^+$  is approximately five times less reactive than  $\text{Pyz}$ . Assuming second-order kinetics, eqs 1, 4b, and 5b were applied for the fit, leading to rate and equilibrium constants

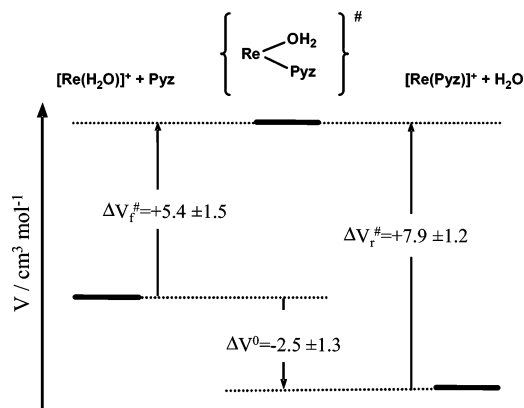


**Figure 6.** Volume profile at 298 K ( $I = 1$  M;  $\text{NaCF}_3\text{SO}_3$ ) for the water substitution on  $[(\text{CO})_3\text{Re}(\text{H}_2\text{O})_3]^+$  (**1**) by  $\text{Pyz}$ .

(Table S5) at variable pressure. For both complex formation reactions, the pressure dependence of the forward and reverse rate constants, as well as the corresponding equilibrium constants, have been fitted to eq 6a–c (Figure S4) leading to the rate constants  $k_f^{298,P}$ ,  $k_r^{298,P}$ , equilibrium constants  $K^{298,P}$ , and activation and reaction volumes  $\Delta V^\ddagger$  and  $\Delta V^\circ$  (Tables S6 and S7). The volume profile corresponding to eq 5b is presented in Figure 6.

$$\ln k_f^{298,P} = \ln k_f^{298,\circ} - \frac{\Delta V_f^\ddagger \times P}{R \times T} \quad (6a)$$

$$\ln k_r^{298,P} = \ln k_r^{298,\circ} - \frac{\Delta V_r^\ddagger \times P}{R \times T} \quad (6b)$$

$$\ln K^{298,P} = \ln \frac{k_f^{298,P}}{k_r^{298,P}} = \ln K^{298,\circ} - \frac{\Delta V^\circ \times P}{R \times T} \quad \Delta V_f^\ddagger - \Delta V_r^\ddagger \quad (6c)$$

**Water Substitution on  $[(\text{CO})_3\text{Re}(\text{H}_2\text{O})_3]^+$  (**1**) by the S-Donor THT Ligand at Variable Pressure.** Complexes of rhenium and osmium with thiophene are well-known and subjects of many investigations as organosulfur-catalyst models of the hydrodesulfurization (HDS) catalytic processes.<sup>18</sup> Thiophene was reported to bind rhenium via either  $\eta^2(\text{C}=\text{C})$  or  $\eta^1(\text{S})$  coordination modes; hence, kinetic measurements of water substitution on **1** were carried out with its fully hydrogenated analogue tetrahydrothiophene THT, by  $^1\text{H}$  NMR.

The reaction of **1** (0.012 M) with THT (0.024 M) was investigated at 298 K in 0.065 M  $\text{CF}_3\text{SO}_3\text{H}$  ( $I = 1$  M;  $\text{NaCF}_3\text{SO}_3$ ). The two triplets of equal intensity (4H) expected for free THT appear at 2.808 and 1.915 ppm attributed, respectively, to the hydrogen atoms of the  $\alpha$  and  $\beta$ , with respect to the S atom, methylene groups (Table S8). After some time, the two signals of the mono-complex  $[(\text{CO})_3\text{Re}(\text{H}_2\text{O})_2(\text{THT})]^+$  (noted  $[\text{Re}(\text{THT})]^+$ ) appear at 3.312 and

(18) (a) Adams, R. D.; Kwon, O.-S.; Perrin, J. L. *J. Organomet. Chem.* **2000**, 596, 102. (b) Brooks, B. C.; Gunnoe, T. B.; Harman, W. D. *Coord. Chem. Rev.* **2000**, 206–207, 3. (c) Rudd, J. A., II; Angelici, R. J. *Inorg. Chim. Acta* **1995**, 240, 393. (d) Arnoldy, P.; Van Oers, A. M.; De Beer, V. H. J.; Moulijn, J. A.; Prins, R. *Appl. Catal.* **1989**, 48, 241.

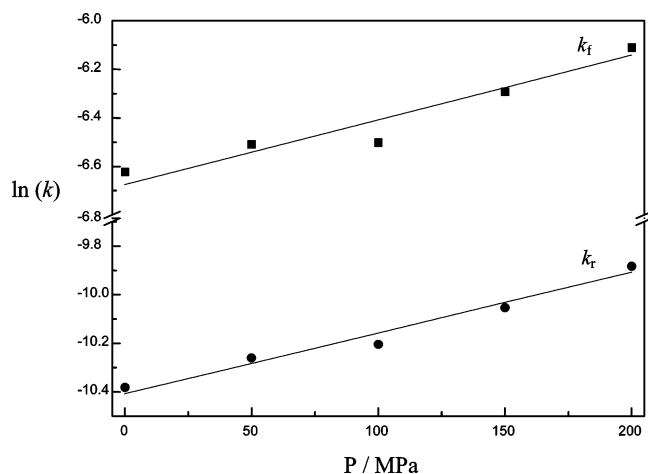


**Figure 7.** Logarithmic plot, as a function of pressure, of the forward and reverse rate constants determined for the formation of  $[\text{Re}(\text{THT})]^+$  at 298 K with solutions containing initially **1** 0.0224 M and THT 0.01 M in  $\text{CF}_3\text{-SO}_3\text{H}$  (0.065 M) ( $I = 1$  M;  $\text{NaCF}_3\text{SO}_3$ ).

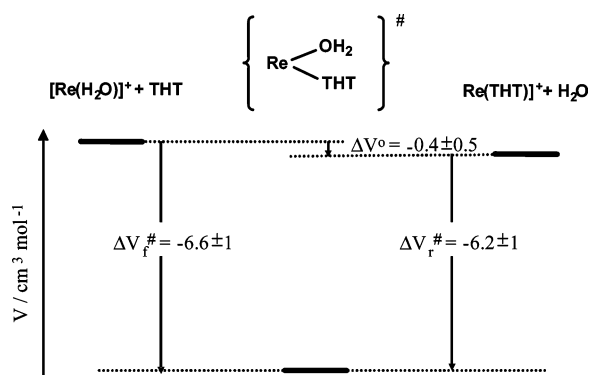
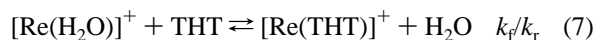
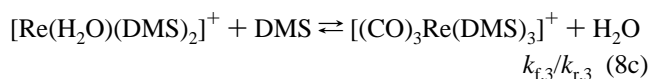
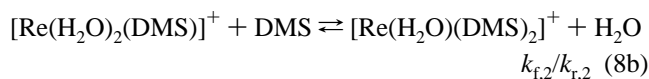
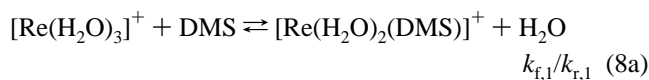


**Figure 8.** Volume profile for the water substitution on  $[(\text{CO})_3\text{Re}(\text{H}_2\text{O})_3]^+$  (**1**) at 298 K ( $I = 1$  M;  $\text{NaCF}_3\text{SO}_3$ ) by THT.

2.109 ppm, followed by the two of the bis-complex  $[(\text{CO})_3\text{Re}(\text{H}_2\text{O})(\text{THT})_2]^+$ , close to the latter, at 3.365 and 2.119 ppm (Figure S5). In order to study the first step only, variable pressure kinetic experiments were conducted by  $^1\text{H}$  NMR (0.1 <  $P$  < 200 MPa), in 0.065 M  $\text{CF}_3\text{SO}_3\text{H}$  ( $I = 1$  M;  $\text{NaCF}_3\text{SO}_3$ ) at 298 K, with a solution of **1** (0.0224 M) with a deficiency of THT (0.01 M), where the bis-complex is not observed at all. Spectra were recorded with time, the signals least-squares fitted as Lorentzians, and the concentrations of each species deduced from the obtained intensities (Figures S6 and S7). Rate and equilibrium constants were determined for each pressure assuming second-order kinetics (eq 7) (Table S9). Then, the  $k_f^{298,0}$ ,  $k_r^{298,0}$ , and  $K^{298,0}$  constants and the activation and reaction volumes  $\Delta V^\ddagger$  and  $\Delta V^\circ$  (Tables S6 and S7) have been calculated using eqs 6a–c (Figure 7). The volume profile corresponding to eq 7 is shown in Figure 8.



**Water Substitution on  $[(\text{CO})_3\text{Re}(\text{H}_2\text{O})_3]^+$  (**1**) by the S-Donor DMS Ligand at Variable Pressure.** As reported previously, dimethyl sulfide (DMS) is able to substitute up to three water molecules on **1**, according to eqs 8a–c (see Figure 9 for concentration profile).<sup>7</sup>



Variable-pressure kinetic measurements (0.1 <  $P$  < 200 MPa) were then performed by  $^1\text{H}$  NMR to determine the activation volumes for the three steps, with solutions of **1** (0.03–0.05 M) and DMS (0.02–0.3 M) at 298 K in 0.1 M  $\text{HBF}_4$  ( $I = 1$  M fixed by  $\text{NaBF}_4$ ) (Table S10). Deduced from the NMR intensities, time dependent concentrations of free DMS and mono-, bis-, and tris-complexes, obtained for the eight experiments, were fitted altogether to eqs 6a–c and eqs 8a–c assuming second-order kinetics. Rate and equilibrium constants  $k_f^{298,0}$ ,  $k_r^{298,0}$ ,  $K^{298,0}$ , and activation and reaction volumes  $\Delta V^\ddagger$ ,  $\Delta V_r^\ddagger$ ,  $\Delta V^\circ$  are collected for the three steps in Table 2 and illustrated by Figure 10, respectively. Since the substitution of the last water molecule is a slow process, the corresponding equilibrium could not be reached under pressure within reasonable experimental time. Therefore, the equilibrium constants were determined at ambient pressure with a sample which was allowed to react for four weeks ensuring completion of the reaction. Equilibrium constants for the three successive steps were determined as  $K_1^{298,0} = 8.3 \pm 0.1 \text{ M}^{-1}$ ,  $K_2^{298,0} = 46.8 \pm 0.8 \text{ M}^{-1}$ ,  $K_3^{298,0} = 52 \pm 6 \text{ M}^{-1}$  and used for the fitting procedure. For the same reason, the activation volume  $\Delta V_{r,3}^\ddagger$  could not be determined accurately and was therefore estimated as  $-3 \pm 5 \text{ cm}^3 \text{ mol}^{-1}$  from  $\Delta V_{r,1}^\ddagger$  and  $\Delta V_{r,2}^\ddagger$ . Supporting this assumption, the fitting procedure, when performed for fixed values of  $\Delta V_{r,3}^\ddagger$  ( $-8$ ,  $-3$ , and  $+2 \text{ cm}^3 \text{ mol}^{-1}$ ), leads only to slight variations, within the standard deviations, in the others parameters (Table S11).

## Discussion

### Rate Constants and Thermodynamics of Complex Formation of $[(\text{CO})_3\text{Re}(\text{H}_2\text{O})_3]^+$ (**1**) with Various Ligands.

The kinetic and thermodynamic results obtained at ambient pressure for the complex formation of **1** with Pyz and THT are consistent with those recently reported with various ligands such as TFA,  $\text{Br}^-$ ,  $\text{CH}_3\text{CN}$ , TU, and DMS (Table 2).<sup>7</sup> All along this range of ligands, the formation rate constant  $k_{f,1}$  increases only by a factor of 3 from the O-donor TFA anion to the N-donors ( $\text{CH}_3\text{CN}$  and Pyz) and then to the S-donors, with the highest value for the thiourea (TU). To allow comparison between charged and uncharged ligands and with the water exchange rate  $k_{\text{ex}}$ , interchange rate constants  $k_i$ 's need to be calculated by dividing the  $k_f$  values by the respective outer-sphere association constants  $K_{\text{OS}}$  and finally to be corrected, for a statistical reason, to give rate constants  $k_i'$ .<sup>19</sup> The interchange rate constant  $k_i'$  for the two

(19) Aebischer, N.; Merbach, A. E. *Inorg. React. Mech.* **1999**, *1*, 233–245.

**Table 2.** Rate and Equilibrium Constants of Complex Formation of [(CO)<sub>3</sub>Re(H<sub>2</sub>O)<sub>3</sub>]<sup>+</sup>, **1**, with Various Ligands L, at *I* = 1 M, *T* = 298 K

L	TFA <sup>a</sup>	Br <sup>-</sup> <sup>a</sup>	CH <sub>3</sub> CN <sup>a</sup>	Pyz <sup>b</sup>	THT <sup>b</sup>	DMS <sup>b</sup>	TU <sup>a</sup>
10 <sup>3</sup> <i>k</i> <sub>f,1</sub> /M <sup>-1</sup> s <sup>-1</sup>	0.81 ± 0.01	1.6 ± 0.3	0.76 ± 0.04	1.06 ± 0.05	1.28 ± 0.07	1.18 ± 0.06	2.49 ± 0.09
10 <sup>3</sup> <i>k</i> <sub>r,1</sub> /s <sup>-1</sup>	99 ± 2	230 ± 100	16 ± 2	0.45 ± 0.04	3.05 ± 0.09	14.2 ± 0.8	1.6 ± 0.2
10 <sup>3</sup> <i>k</i> <sub>f,2</sub> /M <sup>-1</sup> s <sup>-1</sup>						0.76 ± 0.02	4.7 ± 1.7
10 <sup>3</sup> <i>k</i> <sub>r,2</sub> /s <sup>-1</sup>						1.62 ± 0.05	
10 <sup>3</sup> <i>k</i> <sub>f,3</sub> /M <sup>-1</sup> s <sup>-1</sup>						0.106 ± 0.004	5.7 ± 1.2
10 <sup>3</sup> <i>k</i> <sub>r,3</sub> /s <sup>-1</sup>						0.20 ± 0.02	
<i>K</i> <sub>1</sub> /M <sup>-1</sup>	0.82 ± 0.02	0.7 ± 0.3	4.8 ± 0.5	237 ± 15	41 ± 1	8.3 ± 0.1	160 ± 8
<i>K</i> <sub>2</sub> /M <sup>-1</sup>						46.8 ± 0.8	
<i>K</i> <sub>3</sub> /M <sup>-1</sup>						52 ± 6	

<sup>a</sup> From ref 7. <sup>b</sup> This study.**Table 3.** Interchange Rate Constants *k*<sub>i</sub>' for the Water Substitution on [(CO)<sub>3</sub>Re(H<sub>2</sub>O)<sub>3</sub>]<sup>+</sup>, **1**, at *I* = 1 M, *T* = 298 K

L	10 <sup>3</sup> <i>k</i> <sub>f,1</sub> <sup>298</sup> /M <sup>-1</sup> s <sup>-1</sup>	10 <sup>3</sup> <i>k</i> <sub>i</sub> ' a/s <sup>-1</sup>
H <sub>2</sub> O <sup>b</sup>	6.3	6.3
TFA	0.81	2.9
Br <sup>-</sup>	1.6	5.8
CH <sub>3</sub> CN	0.76	12.7
Pyz	1.06	17.7
THT	1.28	21.3
DMS	1.52	22
TU	2.49	41.5

<sup>a</sup> *k*<sub>i</sub>' = (*k*<sub>f,i</sub>)/(*K*<sub>os</sub>*n*<sub>c</sub>) with 1/*f* = probability factor = 1/12, *n*<sub>c</sub> = coordination number = 3, *K*<sub>OS</sub> = 1.1 M<sup>-1</sup> for charged ligands, and *K*<sub>OS</sub> = 0.24 M<sup>-1</sup> for neutral ligands. <sup>b</sup> *k*<sub>ex</sub> = rate constant for the exchange of a particular water molecule.

additional ligands Pyz and THT are collected in Table 3 with those previously reported for various ligands, displaying a discrimination among nucleophiles for complex formation with *k*<sub>i</sub>' ranging from 2.9 × 10<sup>-3</sup> s<sup>-1</sup> for TFA to 41.5 × 10<sup>-3</sup> s<sup>-1</sup> for TU.<sup>7</sup>

The nucleophilic reactivity of the incoming species is often discussed in terms of basicity (toward the proton or water) and polarizability.<sup>20</sup> Here the order of reactivity of the incoming ligand does not correlate with the basicity of that group toward the proton as a consequence of Re(I) being a soft acid, according to Pearson HSAB classification, and H<sup>+</sup> a hard acid. For the specific reaction of **1** with the monoprotonated pyrazine HPyz<sup>+</sup>, the strongly reduced nucleophilic character of the incoming species, in comparison to Pyz, leads to a 26-fold lower rate constant *k*<sub>i</sub>' (Table 1), calculated with the *K*<sub>os</sub> value adequate for charged ligands. However, one can consider that HPyz<sup>+</sup>, of which the charge is opposite to the nucleophilic site, acts more like a neutral ligand, leading therefore to an only 6-fold lower rate constant *k*<sub>i</sub>'. It is noteworthy that the p*K*<sub>a</sub> of pyrazine is decreased when it is bound to the {(CO)<sub>3</sub>Re}<sup>+</sup> moiety since [(CO)<sub>3</sub>Re(H<sub>2</sub>O)<sub>2</sub>(Pyz)]<sup>+</sup> was shown by <sup>1</sup>H NMR spectroscopy to be insensitive to variable acidity, i.e., to protonation. A similar behavior was reported for the [(CN)<sub>5</sub>Ru<sup>II</sup>(PyzH)]<sup>2-</sup> complex, whose p*K*<sub>a</sub> was determined as 0.4, lower than that of free pyrazine (0.6), although the metal–ligand back-donation is expected to increase the basicity of the terminal N site, as in [(NH<sub>3</sub>)<sub>5</sub>Ru<sup>II</sup>(PyzH)]<sup>3+</sup> (p*K*<sub>a</sub> = 2.85). The ancillary π-acceptor ligands CN<sup>-</sup> or CO could be responsible of this effect in [(CN)<sub>5</sub>Ru<sup>II</sup>(PyzH)]<sup>2-</sup> and in **1**, by reducing the electron density at the metal center and limiting by the way its ability to back-donation. Hence in these two complexes, the pyrazine

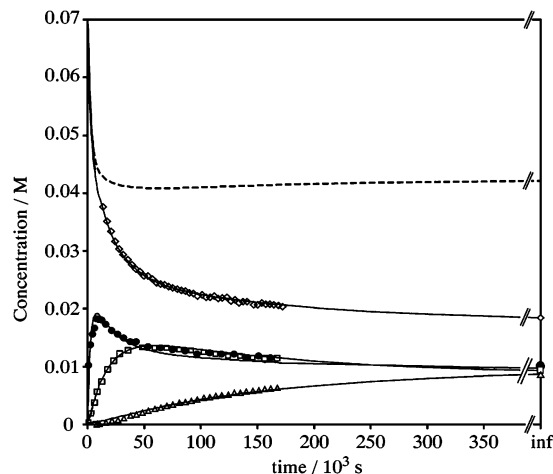


**Figure 9.** Concentration profile as a function of time, at 298 K and 100 MPa, for the reaction between [(CO)<sub>3</sub>Re(H<sub>2</sub>O)<sub>3</sub>]<sup>+</sup> **1** (---) and DMS (○) yielding [(CO)<sub>3</sub>Re(DMS)(H<sub>2</sub>O)<sub>2</sub>]<sup>+</sup> (●), [(CO)<sub>3</sub>Re(DMS)<sub>2</sub>(H<sub>2</sub>O)]<sup>+</sup> (□), and [(CO)<sub>3</sub>Re(DMS)<sub>3</sub>]<sup>+</sup> (△). Initial composition: **1** 0.067 M and DMS 0.072 M in HBF<sub>4</sub> 0.1 M (*I* = 1 M fixed by NaBF<sub>4</sub>).

acts mainly as a σ-donor ligand and causes in turn an increase of its acidity. This statement is also supported by the close *k*<sub>f</sub> values for the reactions of **1** with HPyz<sup>+</sup> or [RePyz]<sup>+</sup> which indicate that the nucleophilicity of the terminal N atom in pyrazine is about the same in both species. Therefore, extrapolating the kinetic nucleophilicity parameter to the thermodynamic basicity parameter, one can conclude that [RePyz]<sup>+</sup> is, to a certain extent, as unlikely to be protonated as is HPyz<sup>+</sup> (p*K*<sub>a1</sub> = -5.8).

Another striking feature of the complex formation of **1** with the studied ligands is the strong increase in *k*<sub>r,1</sub>, the rate constant for the back reaction, from Pyz to Br<sup>-</sup> of 3 orders of magnitude (Table 2). This marked leaving group effect represents the changing nucleofugal ability of each species, which is inversely related to their basic character. According to this statement, bromide (p*K*<sub>a</sub>(HBr) = -4.7) is the fastest leaving group and Pyz (p*K*<sub>a2</sub>(HPyz<sup>+</sup>) = 0.6) the slowest. Consequently, since *k*<sub>r,1</sub> changes to a much lower extent than *k*<sub>f,1</sub>, the equilibrium constants *K*<sub>1</sub> (*K*<sub>1</sub> = *k*<sub>f,1</sub>/*k*<sub>r,1</sub>) of complex formation strongly increase from Br<sup>-</sup> to Pyz. Figure 11 gives the linear plot of log *k*<sub>r,1</sub> versus p*K*<sub>1</sub> with a slope of 0.93 ± 0.07. In agreement with the general principle of a linear free energy relationship, similar correlations were also observed with cobalt(III) and iridium(III) pentaamines with a series of monoanionic ligands.<sup>21</sup> Since Langford pointed out that

(21) (a) Langford, C. H. *Inorg. Chem.* **1965**, *4*, 265. (b) Lamb, A. B.; Fairhall, L. T. *J. Am. Chem. Soc.* **1923**, *45*, 378.

(20) Edwards, J. O. *J. Am. Chem. Soc.* **1954**, *76*, 1540.

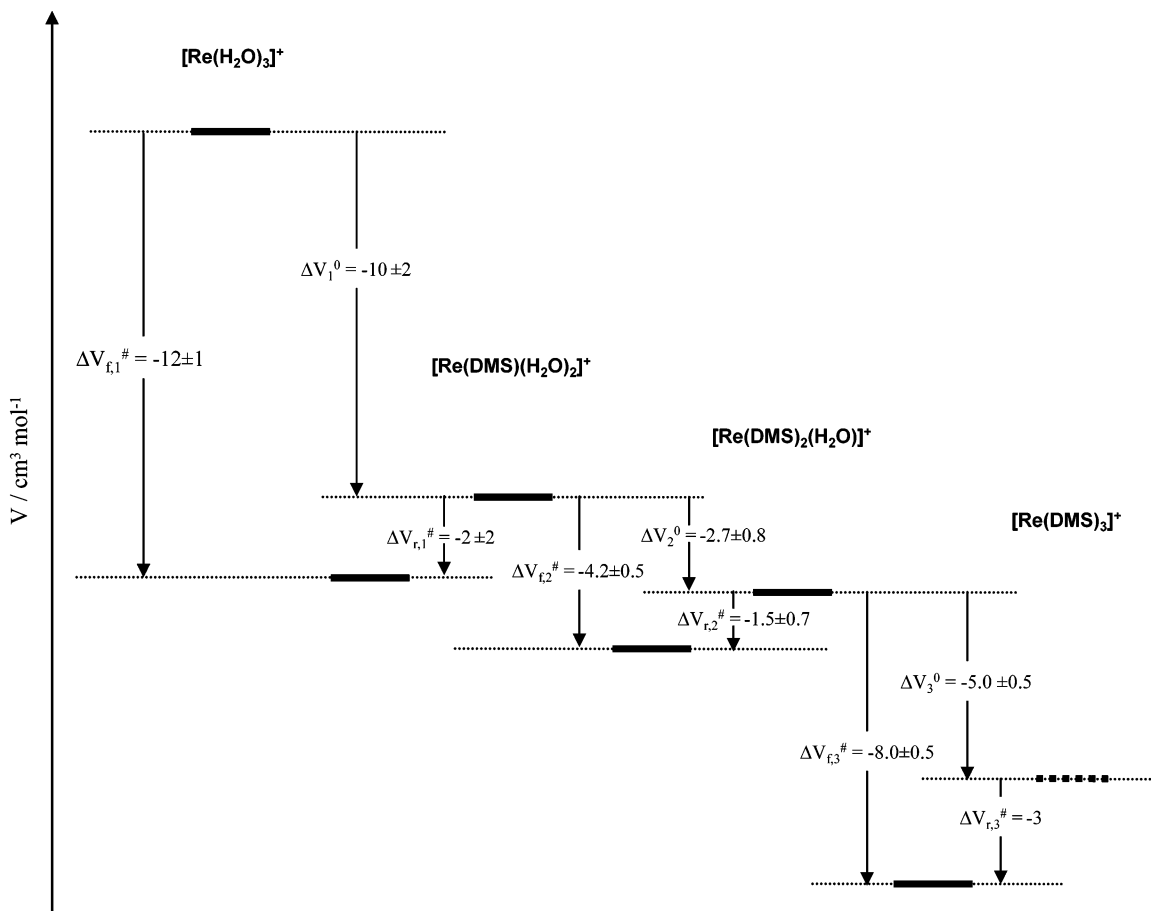


**Figure 10.** Volume profile for the water substitution on  $[(\text{CO})_3\text{Re}(\text{H}_2\text{O})_3]^+$  (1) at 298 K ( $I = 1 \text{ M}$  fixed by  $\text{NaBF}_4$ ) by the DMS (L).

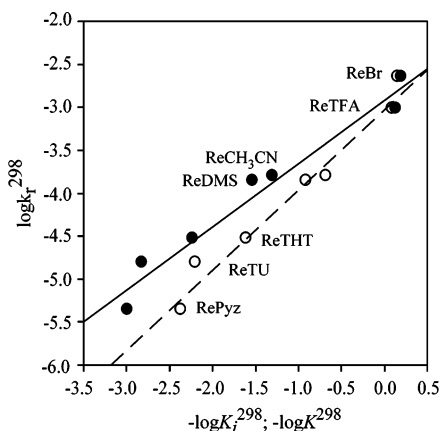


**Figure 11.** Plot of the linear regression of  $\log k_r$  vs  $\text{p}K(\text{O})$  with a slope of  $0.93 \pm 0.07$  and of  $\log k_r$  vs  $\text{p}K_i(\bullet)$  with a slope of  $0.73 \pm 0.06$ .

a slope of 1 for the straight line indicates that the nature of the leaving group in the transition state is about the same as that in the product, namely a solvated species, the authors concluded to a dissociatively activated mechanism. However, Langford pointed to the role of the entering water molecule which is not defined. Moreover, one should be aware that the free energy relationship (slope of 1) means that the rate constant of formation is constant along the series of ligands. It is obviously not the case for the complex formation with 1, although the free energy relationship seems to prevail, since  $k_{r,1}$  varies by a factor of 3 from TFA to TU. Therefore, the complex formation mechanism cannot be thought to be

totally insensitive to the entering ligand, and this is well supported by the large variation by a factor of 14 from TFA to TU of the intrinsic rate constant  $k'_i$ , adequate for comparison of charged and uncharged ligands. From that point of view, it is more appropriate to examine the inversed logarithmic dependence of  $k_{r,1}$ , not versus the global equilibrium constant  $K_1$ , but according to the Eigen–Wilkins mechanism, versus  $K_i$ , the equilibrium constant of the interchange step, i.e., to  $K_1/K_{os}$  ( $K_1/K_{os} = k'_i/k_{r,1}$ ). Hence, this leads to a linear dependence of  $\log k_{r,1}$  versus  $\log K_{os}/K_1$  with a slope of  $0.73 \pm 0.06$  (Figure 11), much less indicative of a dissociative character of the activation, as expected on the basis of formation rate constant  $k_{r,1}$  analysis.

**Volume of Activation for Complex Formation of  $[(\text{CO})_3\text{Re}(\text{H}_2\text{O})_3]^+$  (1).** The water exchange rate  $k_{ex}$  was found close to all the interchange rate constants  $k'_i$  revealing by the way that the rate of complex formation might be limited by rhenium–water bond-breaking, through an  $I_d$  mechanism. However, the discrimination among nucleophiles, even slight, but more than 1 order of magnitude in  $k'_i$ , exists and indicates that the entering ligand could be bound to the rhenium atom in an associative interchange transition state. This ambiguity appears also in the linear free energy graphics with a slope smaller than 1. To describe the transition state on the basis of these elements, one has to have in mind the original Langford–Gray nomenclature<sup>22</sup> which defines the  $I_d$  mechanism, with greatest influence of the leaving group, and the  $I_a$  mechanism with a highest



sensitivity toward the nature of the entering group. Therefore, to make a mechanism assignment, the necessary examination, full of nuances, of the relative roles of the entering/leaving groups can hardly be conducted at this point of the investigations. But essential enlightenment on complex formation mechanism can be provided by activation volumes, from high-pressure experiments. The complex formation of **1** was investigated at variable pressure with neutral S-donor ligands DMS and THT, and the N-donor Pyz ligand. The activation volumes  $\Delta V_{f,1}^\ddagger$  and  $\Delta V_{r,1}^\ddagger$ , obtained for monocomplex formation with these three species (Figures 6, 8, and 10), instead of settling on one particular  $I_d$  or  $I_a$  mechanism, clearly suggest the existence of both from the observed changes in  $\Delta V^\ddagger$  sign, from positive to negative, when going from the harder Pyz ( $\Delta V_{f,1}^\ddagger = +5.4 \pm 1.5$  and  $\Delta V_{r,1}^\ddagger = +7.9 \pm 1.2$   $\text{cm}^3 \text{mol}^{-1}$ ) to the softer THT ( $\Delta V_{f,1}^\ddagger = -6.6 \pm 1$  and  $\Delta V_{r,1}^\ddagger = -6.2 \pm 1$   $\text{cm}^3 \text{mol}^{-1}$ ) and DMS ( $\Delta V_{f,1}^\ddagger = -10 \pm 2$  and  $\Delta V_{r,1}^\ddagger = -6 \pm 2$   $\text{cm}^3 \text{mol}^{-1}$ ). Hence, the mechanism of complex formation of **1** seems to be dual, changing from an  $I_d$  mechanism, occurring when discrimination between water and the entering ligand is poor, toward an  $I_a$  mechanism with best nucleophiles. However, according to the Eigen–Wilkins mechanism, the observed activation volume  $\Delta V_{\text{obs}}^\ddagger$  consists of an intrinsic activation volume  $\Delta V_1^\ddagger$  for interchange and a solvation one  $\Delta V_{\text{solv}}^\ddagger$  (eq 9).

$$\Delta V_{\text{obs}}^\ddagger = \Delta V_{\text{solv}}^\ddagger + \Delta V_1^\ddagger \quad (9)$$

Since DMS ( $\text{p}K_{\text{ow}} = 0.8 \pm 0.3$ ) and THT ( $\text{p}K_{\text{ow}} = 1.2 \pm 0.4$ ) are hydrophobic molecules<sup>23</sup> whereas Pyz is hydrophilic ( $\text{p}K_{\text{ow}} = -0.26$ ),<sup>24</sup> one can legitimately wonder to what extent the expected difference in solvation of both types of ligands can affect the  $\Delta V_{\text{solv}}^\ddagger$  and finally the  $\Delta V_{\text{obs}}^\ddagger$ . However, the answer can easily be found in the negative reaction volumes  $\Delta V^\circ$ , with no particular trend from pyrazine ( $\Delta V_1^\circ = -2.5 \pm 1.3$   $\text{cm}^3 \text{mol}^{-1}$ ) to THT and DMS ( $\Delta V_1^\circ = -0.4 \pm 0.5$  and  $\Delta V_1^\circ = -10.0 \pm 2$   $\text{cm}^3 \text{mol}^{-1}$  respectively), indicating the minor solvation contribution to  $\Delta V^\circ$  and then to  $\Delta V_{\text{obs}}^\ddagger$ . Hence,  $\Delta V_{\text{obs}}^\ddagger$  is mainly due to structural differences between the transition and the initial states, and the volume profiles can unambiguously be interpreted as indicative of an  $I_d$ , for Pyz, and an  $I_a$  mechanism for THT and DMS.

Finally, the reaction between **1** and DMS involves the successive formation of the mono-, bis-, and trisdimethyl-

sulfide complexes with rate, equilibrium constants, and activation volumes for each step. Table 2 shows that increasing substitution is paralleled by a decrease of the successive complex formation rates. This kinetic trend, related to increased steric hindrance on the metal center, and the volume profile are conclusive for an associatively activated substitution mechanism. Conversely, with the less bulky thiourea (smaller cone angle), an increase in the rate constants is observed with growing substitution. This may be explained by the softening of the metal center by the already coordinated ligand, therefore exhibiting a higher affinity for soft ligands. This symbiotic effect also explains the increase of the equilibrium constants with DMS upon successive coordination which seem at first sight to be in contradiction with the slow of  $k_f$  due to crowding. Such softening of a metal center by coordinated ligands is well illustrated by the Nb(V) and Ta(V) pentachlorocomplexes which exhibit a high affinity for soft ligands such as the series of dimethyl chalcogenides (S, Se, Te) although the naked  $\text{Nb}^{5+}$  and  $\text{Ta}^{5+}$  ions are very hard acids.<sup>25</sup>

## Conclusion

The study of complex formation of **1** with various ligands showed that its rate can be affected by the entering group with intrinsic formation rate constants  $k_f'$  ranging from  $2.9 \times 10^{-3}$  (TFA) to  $41.5 \times 10^{-3} \text{ s}^{-1}$  (TU). Nevertheless,  $k_f'$  values remain close to that of water exchange  $k_{\text{ex}}$  and were interpreted to be indicative of a dissociatively activated mechanism; however, it was mentioned that the moderate increase of  $k_f'$  with the S-donor ligands could suggest a slight deviation of the mechanism toward a more associative one for this last category of ligands.<sup>7</sup> With the help of activation volumes, this mechanistic ambivalence was clearly revealed as a specificity of the complex formation reactions of **1**. With hard nucleophiles, such as O- and N-donors, the  $I_d$  mechanism prevails with a bond-breaking limiting step. The greater affinity of soft S-donor nucleophiles for the soft rhenium center leads these ligands to be involved in an associative transition state, according to an  $I_a$  mechanism.

**Acknowledgment.** We thank Fabrice Yerly for his assistance in using the Visualiseur/Optimiseur software. Financial support by the Swiss National Science Foundation and COST B12 is gratefully acknowledged. The cartoons in the cover artwork are from Dirk Pubanz.

**Supporting Information Available:** Additional tables and figures. This material is available free of charge via the Internet at <http://pubs.acs.org>.

IC034969A

(22) Langford, C. H.; Gray, H. B. *Ligand Substitution Processes*; W. A. Benjamin Inc.: New York, 1965.

(23) Calculated using Advanced Chemistry Development (ACD) Software Solaris V4.67; ACD, 1994–2003.

(24) Hansch, C.; Leo, A.; Hoekman, D.; Heller, S. R. *Hydrophobic, Electronic, and Steric Constants*; American Chemical Society: Washington, DC, 1995.

(25) Good, R.; Merbach, A. E. *Inorg. Chem.* **1974**, *14*, 1030–1034.